Research Journal of Applied Sciences, Engineering and Technology 7(1): 49-55, 2014
DOI:10.19026/rjaset.7.219
ISSN: 2040-7459; e-ISSN: 2040-7467

Submitted: January 25, 2013 Accepted: February 25, 2013 Published: January 01, 2014

Research Article

Implementation of Galerkin's Method and Modal Analysis for Unforced Vibration Response of a Tractor Suspension Model

[1]Ramin Shamshiri and [2]Wan Ishak Wan Ismail
[1]Department of Agricultural and Biological Engineering, University of Florida, Gainesville, FL 32611, USA
[2]Department of Biological and Agricultural Engineering, Universiti Putra Malaysia, Serdang, Selangor, Malaysia

Abstract: This study provides a numerical tool for modeling and analyzing of a two degree of freedom suspension system that is used in farm tractors. In order to solve the corresponding coupled system of equations, dynamic modal expansion method and matrix transformation technique were first used to formulate the problem and to obtain the natural frequencies and modes of the tractor rear axle suspension. Galerkin's method over the entire time domain was then employed to analyze the modal equation of motion for the unforced response. It was shown through calculations that the algorithm over entire time domain could not be generalized for computer implementation. In order to develop a stand-alone algorithm implementable in any programming environment, Galerkin's method was applied over smaller elements of time domain. The modal and vertical equations of motions describing the suspension system were then solved numerically for both with and without damping cases. The program was used successfully to solve the actual coupled equations and to plot the results. Finally, for the damped case, where stability of the system was expected, the numerical results were confirmed through Lyapunov stability theorem.

Keywords: Galerkin's method, modal analysis, numerical method, tractor suspension, unforced vibration

INTRODUCTION

Suspension systems are necessary to improve ride comforts and to reduce vibrations that are harmful to health and deleterious to performance for the driver of an agricultural tractor. A research conducted by Lines *et al*. (1995) on whole tractor body during driving has compared unsuspended and suspended transmitted vibrations during different tasks and concluded that transports involve the highest vibration level and risk for the driver's safety. The subject of the transmitted vibrations of agricultural tractors to the driver and measuring the behavior of the seat vibrations has been widely discussed over the last 50 years (Rossegger and Rossegger, 1960; Matthews, 1964, 1977; Stayner, 1976; Mothiram and Palanichamy, 1985; Deboli and Potecchi, 1986, Park and Stott, 1990; Hansson, 1996; Mehta and Tewari, 2000; Scarlett *et al*., 2007; Servadio *et al*., 2007; Mehta *et al*., 2008). Experiments for improving tractor operator ride and optimization of the cabin suspension parameters have been studied by Hilton and Moran (1975), Hansson (1995), Marsili *et al*. (2002), Thoresson (2003) and Zehsaz *et al*. (2011). In farm tractors, the reason for free vibrations of the suspension system is due to the condition that these machines are subjected to work, which intensify transferring back and forth of the kinetic energy, in the suspension mass and the potential energy in the springs. It is therefore of interest to study this system when it is set off with an initial input which causes free vibrations at its natural frequency and then damp down to zero. It should be noted that this case is different from the forced vibration where the frequency of the vibration is the frequency of the applied force and with order of magnitude being dependent on the actual mechanical system.

Various analytical approaches have been already utilized to extend tractor ride simulation and mathematical models for minimization of vibration responses (Stayner, 1972; Stayner *et al*., 1984; Patil and Palanichamy, 1988; Lehtonen and Juhala, 2006; Yang *et al*., 2009; Kolator and Białobrzewski, 2011). With the aim of providing improved isolation from vibrations on more than one axis in farm tractors, the development of more sophisticated suspension systems lead to more complex dynamic coupled initial or boundary value problems which can be solved with numerous available computer tools, such as MATLAB® (The MathWorks Inc, Natick, MA) ode45 or bvp4c built-in functions, however, in either case, these equation must be first reduced into an equivalent system of first-order ordinary differential equations. This step is necessary

Corresponding Author: Ramin Shamshiri, Department of Agricultural and Biological Engineering, University of Florida, Gainesville, FL 32611, USA

because for example, MATLAB uses a variable step Runge-Kutta (Dormand and Prince, 1980) method for ode45 and three-stage LobattoIIIa formula (Shampine *et al*., 2000) for bvp4c to solve differential equations numerically, which is valid only for first order equations. This routine creates a limitation for writing a general computer algorithm since it requires the system of first order differential equations to be analytically updated each time as dynamics of the original suspension model changes (Roy and Andrew, 2011).

As an alternative numerical approach for solving complex differential equations, Galerkin's Method (Kantorovich and Krylov, 1964) is widely used, especially for problems to which no analytical function exists or is known to exist. Some of the applications of Galerkin's method through few numbers of trial functions over entire time domain have been discussed for agricultural engineering problems by Carson *et al*. (1979).

Since the original dynamic equation of the tractor suspension system was coupled, the Vertical Equations of Motion (VEOM) in physical coordinates were first projected onto modal coordinates using eigenvalues and eigenvectors that were resulted from solving the un-damped frequency eigen-problem. Galerkin's method was then employed for solving the two uncoupled modal equations independently. It was shown that as the number of trial functions to approximate the modal equation increases in Galerkin's method over the entire time domain, the power of terms starts growing and therefore makes this method unsuitable for implementation as a generalized algorithm. To develop a stand-alone algorithm that could be generalized for this problem and also implementable in any programming environment, Galerkin's method was applied over adjustable same-sizes smaller elements of time domain. It was proven and shown that this modification provides a flexible and general numerical tool for implementation in computer simulation and successfully solved the two uncoupled modal equations numerically for both with and without damping cases. Finally the numerical results from modal equations were transformed back to physical coordinates and superpose to produce the response of the actual suspension system.

MATERIALS AND METHODS

An active suspension model of tractor is shown schematically in Fig. 1. We consider the two Degree of Freedom (DOF) mass-spring and shock absorber dynamic system where m_1 and m_2 are the tractor mass and the suspension mass in (kg), x_s and x_w are the displacement of tractor body in (m) and the suspension mass, k_1 and k_2 are the spring coefficients in $(N.m^{-1})$ and b_1 and b_2 are the damper coefficients in $(N.s.m^{-1})$. Based on Newton's law, the two VEOM describing this system are given in (1) and (2). The inputs of the systems are the control force u from the actuator and the field disturbance r. For the purpose of free vibration analysis, we ignore the control force and disturbance effects and then reproduce the VEOM in matrix notation as given by the following boundary value problem in (3):

$$m_1 \frac{d^2x_s}{dt^2} - b_1\left(\frac{dx_w}{dt} - \frac{dx_s}{dt}\right) - k_1(x_w - x_s) - u = 0 \quad (1)$$

$$m_2 \frac{d^2x_w}{dt^2} - b_1\left(\frac{dx_s}{dt} - \frac{dx_w}{dt}\right) - k_1(x_s - x_w) - b_2\left(\frac{dr}{dt} - \frac{dx_w}{dt}\right) - k_2(r - x_w) + u = 0 \quad (2)$$

$$\boldsymbol{M\ddot{x} + B\dot{x} + Kx} = 0 t_1 \le t \le t_2$$
$$BC: x_s(t_1) = x_{s1}, \quad x_s(t_2) = x_{s2}, \quad x_w(t_1) = x_{w1}, \quad x_w(t_2) = x_{w2} \quad (3)$$

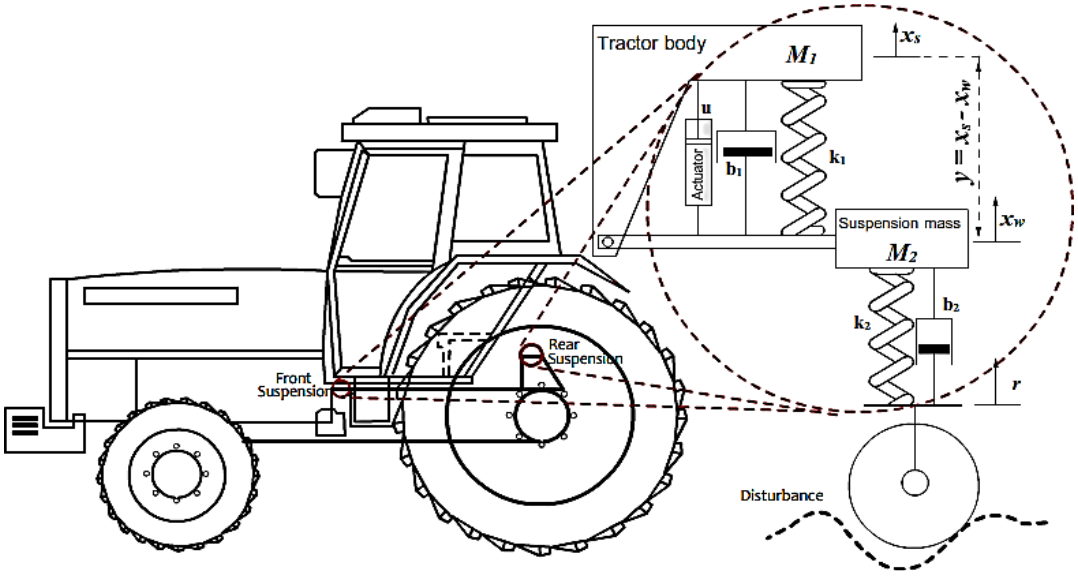

Fig. 1: Schematic diagram of a tractor model and its active suspension system

where, $\boldsymbol{M} = \begin{bmatrix} m_1 & 0 \\ 0 & m_2 \end{bmatrix}$, $\boldsymbol{B} = \begin{bmatrix} b_1 & -b_1 \\ -b_1 & b_1 + b_2 \end{bmatrix}$ and $\boldsymbol{K} = \begin{bmatrix} k_1 & -k_1 \\ -k_1 & k_1 + k_2 \end{bmatrix}$ are the suspension mass, damper and spring coefficients matrix, respectively, $\mathbf{x}$, $\dot{\mathbf{x}}$ and $\ddot{\mathbf{x}}$, $\in R^{2\times1}$, are the displacement, velocity and acceleration vectors. Furthermore, it can be seen that M, B and K are symmetric, $\boldsymbol{M}$ is Positive Definite (PD) whereas K is nonnegative definite. As a consequence of these properties, the natural frequencies (in Hz unit, ω_1 and ω_2) of the two-DOF suspension system shown in Fig. 1, undergoing in-phase harmonic motions, will be nonnegative and real. These natural frequencies can be determined by solving the characteristic polynomial of the free-vibration eigen-problem, $\mathbf{K}.\mathbf{X_i} = \omega_i^2\,\mathbf{M}$ associated with Eq. (3). Here, $i = 1, 2$ stands for natural frequency index and $\mathbf{X} = [\mathrm{X}_1 \quad \mathrm{X}_2]$ is a nonzero 2-eigenvector matrix that has the amplitudes of the motions, $\mathbf{x(t)} = [x_s(t) = \mathrm{X}_1.f(t) \quad x_w(t) = \mathrm{X}_2.f(t)]^{\mathrm{T}}$ of the suspension masses as entries. Each eigenvector $\mathbf{X_i}$ are scaled through $\mathbf{X_i} = c_i\phi_i$ where ϕ_i is the notation for the i^{th} normal mode and c_i is the scaling factor chosen according to unit largest entry eigenvector normalization criteria described by Roy and Andrew (2011). The modal masses and stiffnesses associated with the modes $\phi_1$and ϕ_2 are calculated through $M_{\mathrm{i}} = \phi_i^T\mathbf{M}\phi_i$ and $K_{\mathrm{i}} = \phi_i^T\mathbf{K}\phi_i$ respectively. In order to get unit generalized masses, modes ϕ_i are renormalized through $\tilde{\phi}_i = c_i'\phi_i$ where c_i' are found by solving $\tilde{\phi}_i^T\mathbf{M}\tilde{\phi}_i = 1$. The two-DOF displacement vector $\mathbf{x(t)}$ is then expressed in terms of normal coordinates $\eta(t)$ as: $x_i(t) = \sum_{i=1}^{2}\phi_i\eta_i(t) = \mathbf{\Phi\eta}$ where $\mathbf{\Phi} = [\tilde{\phi}_1 \quad \tilde{\phi}_2]$ is the modal matrix and $x_1(t)$ and $x_2(t)$ are $x_s(t)$ and $x_w(t)$ respectively. The generalized mass ($\mathbf{M_g}$), damping ($\mathbf{B_g}$) and stiffness ($\mathbf{K_g}$) are defined as $\mathbf{M_g} = \mathbf{\Phi^T M\,\Phi = I}$, where $\mathbf{I}$ is the identity matrix, $\mathbf{B_g} = \mathbf{\Phi^T B\,\Phi}$ and $\mathbf{K_g} = \mathbf{\Phi^T K\,\Phi} = \mathrm{diag}\,(\omega_i^2)$. Since the generalized damping matrix is not diagonal, the resulting modal VEOM for the damped system will not decouple. To resolve this problem, Rayleigh quotient (Nocedal and Wright, 2006) diagonalization technique was applied. The entries of the diagonalized $\mathbf{B_g}$ matrix are calculated through $B_i = \phi_i^T\mathbf{B}\phi_i/\phi_i^T\phi_i$. The effective modal damping factors are also calculated through $\boldsymbol{\zeta_i} = \mathbf{B_{g_i}}/\mathbf{2}\omega_i$. The two decoupled solvable modal equations of motion with boundary conditions are given in (4 and 5):

$$M_{g_1}\ddot{\eta}_1(t) + B_1\dot{\eta}_1(t) + \omega_1^2\eta_1(t) = 0,$$

$$BC: \eta_{11}(t_1) = \Phi^{\mathrm{T}}\,\mathrm{M}\,x_{s1},\ \eta_{12}(t_1) = \Phi^{\mathrm{T}}\,\mathrm{M}\,x_{s2} \quad (4)$$

$$M_{g_2}\ddot{\eta}_2(t) + B_2\dot{\eta}_2(t) + \omega_2^2\eta_2(t) = 0,$$

$$BC: \eta_{21}(t_1) = \Phi^{\mathrm{T}}\,\mathrm{M}\,x_{w1},\ \eta_{22}(t_1) = \Phi^{\mathrm{T}}\,\mathrm{M}\,x_{w2} \quad (5)$$

These two modal equations are first solved numerically through Galerkin's method over the entire domain $[t_1, t_2]$. For the sake of convenience in elaborating the technique, the index 1 and 2 is omitted from Eq. (4) and (5). We let $M_g\ddot{\tilde{\eta}} + B_g\dot{\tilde{\eta}} + \omega\tilde{\eta} = R(t)$, where $R(t)$ is the residual function. This will result a continuous function in the form of summation of some polynomials that are not linear. The approximate solution $\tilde{\eta}(t)$ is expressed as a sum of trial functions in the form of $\tilde{\eta}(t) = \sum_{i=1}^{n} a_i u_i\,(t)$ where n is the number of term used, $u_i(t)$ are known trial functions and a_i are coefficients to be determined using the weighted residual method. The Galerkin's method differs from other weighted residual methods in that the n weighted functions are same as the n number of trial function, $u_i(t)$. Thus we obtain the n number of weighted residual equations as: $\int_{t_1}^{t_2} R(t)u_i(t)dt = 0, i = 1, \ldots, n$, which solving yields:

$$\begin{aligned} -M_g\int_{t_1}^{t_2}\frac{du_i}{dt}\sum_{j=1}^{n}a_j\frac{du_j}{dt}dt + B_g\int_{t_1}^{t_2}u_i(t)\sum_{j=1}^{n}a_j\frac{du_j}{dt}dt \\ + \omega\int_{t_1}^{t_2}u_i(t)\sum_{j=1}^{n}a_j\,u_j dt \\ = M_g[\dot{\eta}(t_1)u_i(t_1) - \dot{\eta}(t_2)u_i(t_2)] \end{aligned}$$

$$[\boldsymbol{\mathcal{K}}]_{n\times n}\{\mathbf{A}\}_{n\times1} = \{\boldsymbol{\mathcal{F}}\}_{n\times1} \quad (6)$$

where, $\boldsymbol{\mathcal{K}} = \left(-M_g[\boldsymbol{\mathcal{K}}_1] + B_g[\boldsymbol{\mathcal{K}}_2] + \omega[\boldsymbol{\mathcal{K}}_3]\right)$, $\boldsymbol{\mathcal{K}}_{1_{ij}} = \int_{t_1}^{t_2}\frac{du_i}{dt}\frac{du_j}{dt}dt$, $\boldsymbol{\mathcal{K}}_{2_{ij}} = \int_{t_1}^{t_2}\phi_i\frac{du_j}{dt}dt$ $\boldsymbol{\mathcal{K}}_{3_{ij}} = \int_{t_1}^{t_2}u_i u_j\,dt$ and $\boldsymbol{\mathcal{F}}_i = M_g[\dot{\eta}(t_1)u_i(t_1) - \dot{\eta}(t_2)u_i(t_2)]$. By considering $\tilde{\eta}(t) = \sum_{i=1}^{n}a_i\eta^i\,(t)$ as the trial function, the elements of the $\boldsymbol{\mathcal{K}}$ matrix are given through formula in (7). The implementation of this method for the given trial function has been provided in Table 1. It can be seen that the ascending power of the terms in the elements of the $\boldsymbol{\mathcal{K}}$ matrix depends on the number of terms in the trial function. In addition, selection of the different trial function will result in a different solution which is considered a drawback for a general implementation:

$$\begin{aligned} \left[\mathcal{K}_{i\times j}\right]_{n\times n} = \left(-M.(i.j).\frac{t_2^{j+i-1} - t_1^{j+i-1}}{i+j-1}\right) \\ + \left(B.j.\frac{t_2^{i+j} - t_1^{i+j}}{i+j}\right) \\ + \left(\omega.\frac{t_2^{i+j+1} - t_1^{i+j+1}}{i+j+1}\right) \\ i, j = 1, \ldots, n \end{aligned} \quad (7)$$

To generalize this method for numerical implementation, we first consider (n_e) individual same l_e size elements of time domain. In this approach, a general element, e that has two nodes, i and j such that:

Table 1: Implementation of Galerkin's method over entire time domain, for solving Eq. (4) and (5) with "$\boldsymbol{n}$" trail functions

Pseudo code and description
Building overall $\mathcal{K}$ matrix
$for\ i = 1{:}n$ {n: *Number of trial functions*}
$for\ j = 1{:}n$
$\mathcal{K}_1$ *matrix corresponding to the* $\ddot{\eta}$
$\mathcal{K}_{1_{i,j}} = (i.j).(t_2^{j+i-1} - t_1^{j+i-1})/(i+j-1);$
$\mathcal{K}_2$ *matrix corresponding to the* $\dot{\eta}$
$\mathcal{K}_{2_{i,j}} = j.(t_2^{i+j} - t_1^{i+j})/(i+j);$
$\mathcal{K}_3$ *matrix corresponding to the* η
$\mathcal{K}_{3_{i,j}} = (t_2^{i+j+1} - t_1^{i+j+1})/(i+j+1);$
end
end
$\mathcal{K} = -M_g.\mathcal{K}_1 + B_g.\mathcal{K}_2 + \omega^2.\mathcal{K}_3;$ {*Overall* $\mathcal{K}$ *matrix*}
Building $\mathcal{K}_S$ *matrix for* $n \times n$ *system of equations*
$for\ i = 1{:}n-1$
$for\ j = 1{:}n$
$\mathcal{K}_{S_{i,j}} = \mathcal{K}_{i,j} + (j.M_g.t_2^{j+i-1} - j.M_g.t_1^{j+i-1});$
end
end
$for\ j = 1{:}n$
$\mathcal{K}_{S_{n-1,j}} = t_1^j;$
$\mathcal{K}_{S_{n,j}} = t_2^j;$
end
$for\ i = 1{:}n-1$
$\mathcal{F}_{i,1} = 0;$
end
$\mathcal{F}_{n-1,1} = \eta_1;$ {*Applying boundary conditions* }
$\mathcal{F}_{n,1} = \eta_2;$
$[A] = [\mathcal{K}_S]^{-1}.[\mathcal{F}];$ {a_i: *Coefficients of terms*}
$t = t_1{:}dt{:}t_2;$ {$t_1 \le t \le t_2$}
$for\ i = 1{:}(t_2 - t_1)/dt + 1$
{Calculating$\tilde{\eta}(t) = \sum_{i=1}^{n} a_i u_i(t)$}
$for\ j = 1{:}n$
$\eta_i = \eta_i + A_{j,1}.t_i^j;$
end
end
$for\ i = 1{:}n$
$d\eta_i = (\eta_{i+1} - \eta_i)/l_e;$ {Calculating $\dot{\eta}$}
end
$for\ i = 2{:}n$
$d^2\eta_i = (d\eta_{i+1} - d\eta_i)/l_e;$ {Calculating$\ddot{\eta}$}
end

$t_j > t_i$ is first considered. In order to apply Galerkin's method to one element at a time, a local coordinate ξ such that $\xi = 0$ at node i and $\xi = 1$ at node j is introduced. The relation between t and ξ for element e is then: $t = t_i + \xi(t_j - t_i)$, where $t_j - t_i = l_e$. The approximate solution within the element e can be given by: $\tilde{\eta}(t) = \eta_i N_1(t) + \eta_j N_2(t)$, where N_1 and N_2 are the interpolation functions and can be expressed as a function of the variable ξ as $N_1(\xi) = 1 - \xi$ and $N_2(\xi) = \xi$. The derivatives of N_i are then $dN_1/dt = -1/l_e$ and $dN_2/dt = 1/l_e$. It can be seen that the interpolation functions satisfy the required relations: $N_1(t_i) = 1, N_1(t_j) = 0, N_2(t_i) = 0, N_1(t_j) = 1$. In this formulation, $\tilde{\eta}(t_i) = \eta_i$ and η_j are nodal solution at nodes i and j, respectively, the derivative of $\tilde{\eta}(t)$ is obtained as: $d\tilde{\eta}/dt = 1/l_e \begin{bmatrix} \frac{dN_1}{d\xi} & \frac{dN_2}{d\xi} \end{bmatrix} \begin{Bmatrix} \eta_1 \\ \eta_2 \end{Bmatrix}$. Applying the Galerkin method at the element level yields: $\int_{t_i}^{t_j} (M_g \ddot{\tilde{\eta}} + B_g \dot{\tilde{\eta}} + \omega \tilde{\eta}) N_i(t) dt = 0$. Using integration by part, to reduce the order of differentiation of $\tilde{\eta}$ and then changing the variable t to ξ by substituting $d\tilde{\eta}/dt$ and dN_i/dt and replacing integration domain by using the relation: $dt = l_e d\xi$, we obtain the following compact form solution in (8):

$$\begin{aligned} &\tfrac{M_g}{l_e} \int_0^1 \left(\begin{Bmatrix} dN_1/d\xi \\ dN_2/d\xi \end{Bmatrix} \begin{bmatrix} \frac{dN_1}{d\xi} & \frac{dN_2}{d\xi} \end{bmatrix} \begin{Bmatrix} \eta_1 \\ \eta_2 \end{Bmatrix} \right) d\xi - \\ &B_g \int_0^1 \left(\begin{Bmatrix} N_1(\xi) \\ N_2(\xi) \end{Bmatrix} \begin{bmatrix} \frac{dN_1}{d\xi} & \frac{dN_2}{d\xi} \end{bmatrix} \begin{Bmatrix} \eta_1 \\ \eta_2 \end{Bmatrix} \right) d\xi - \\ &\omega l_e \int_0^1 \left(\begin{Bmatrix} N_1(\xi) \\ N_2(\xi) \end{Bmatrix} . [N_1(\xi) \quad N_2(\xi)] \begin{Bmatrix} \eta_1 \\ \eta_2 \end{Bmatrix} \right) d\xi = \\ &M_g \left(\dot{\eta}(t_j) N_i(1) - \dot{\eta}(t_i) N_i(0) \right) \\ &\left[\boldsymbol{\mathcal{K}}^{(e)} \right]_{2\times 2} . \{\boldsymbol{\eta}\}_{2\times 1} = \{\boldsymbol{\mathcal{F}}\}_{2\times 1} \end{aligned} \tag{8}$$

Here, $\left[\boldsymbol{\mathcal{K}}^{(e)}\right]_{2\times 2} = \left(M_g \left[\boldsymbol{\mathcal{K}}_1^{(e)}\right] - B_g \left[\boldsymbol{\mathcal{K}}_2^{(e)}\right] - \omega \left[\boldsymbol{\mathcal{K}}_3^{(e)}\right] \right)$, $\{\boldsymbol{\eta}\} = \begin{Bmatrix} \eta_i \\ \eta_j \end{Bmatrix}$ and $\{F\} = \begin{Bmatrix} -\dot{\eta}(t_i) \\ \dot{\eta}(t_j) \end{Bmatrix}$. The values of matrices corresponding to mass, damper and spring were calculated as follow:

$$\left[\boldsymbol{\mathcal{K}}_1^{(e)}\right]_{2\times 2} = \left(\frac{1}{l_e}\right) \int_0^1 \begin{bmatrix} \left(\frac{dN_1}{d\xi}\right)^2 & \left(\frac{dN_1}{d\xi}\right)\left(\frac{dN_2}{d\xi}\right) \\ \left(\frac{dN_2}{d\xi}\right)\left(\frac{dN_1}{d\xi}\right) & \left(\frac{dN_2}{d\xi}\right)^2 \end{bmatrix} d\xi = (1/l_e)[1 \quad -1 \quad ; \quad -1 \quad 1]$$

$$\left[\boldsymbol{\mathcal{K}}_2^{(e)}\right]_{2\times 2} = \int_0^1 \begin{bmatrix} \frac{N_1(\xi) dN_1}{d\xi} & \frac{N_1(\xi) dN_2}{d\xi} \\ \frac{N_2(\xi) dN_1}{d\xi} & \frac{N_2(\xi) dN_2}{d\xi} \end{bmatrix} d\xi = [-1/2 \quad 1/2 \quad ; \quad -1/2 \quad 1/2]$$

$$\left[\boldsymbol{\mathcal{K}}_3^{(e)}\right]_{2\times 2} = l_e \int_0^1 \begin{bmatrix} (N_1(\xi))^2 & N_1(\xi).N_2(\xi) \\ N_2(\xi).N_1(\xi) & (N_2(\xi))^2 \end{bmatrix} d\xi = l_e[1/3 \quad 1/6 \quad ; \quad 1/6 \quad 1/3]$$

It should be noted that we do not need to convert $\tilde{\eta}(t_j)$ and $\tilde{\eta}(t_i)$ because the boundary conditions do not use the approximation scheme. This equation is derived for each element $e = 1, 2, \ldots, n_e$ where n_e is the number of elements. The right hand side of these equations contain terms that are derivatives at the nodes $\dot{\eta}(t_i)$ and $\dot{\eta}(t_j)$ which are not generally known, however the second equation for the element (e) can be added to the first equation of element $(e+1)$ to eliminate the derivative term. Continuing this process for successive elements and the $2 \times n_e$ equations for the n_e elements will reduce to $n_e + 1 = n_d$ number of equations which is equal to the number of nodes. The n_d equations to be solved take the following form in (9) where $\mathcal{K}_{Glob}$ is the global stiffness matrix.The implementation of this method has been provided in Table 2.

Table 2: Implementation of Galerkin's method over "ne" individual time elements, for solving Eq. (4) and (5)

Pseudo code and description
Defining time element length
$l_e = (t_2 - t_1)/n_e;$
Defining time increments
$t = t_1 : l_e : t_2;$
$\mathcal{K}_1$ *matrix corresponding to the* $\ddot{\eta}$
$\mathcal{K}_1^{(e)} = M_g/l_e \,.[1, -1; -1, 1];$
$\mathcal{K}_2$ *matrix corresponding to the* $\dot{\eta}$
$\mathcal{K}_2^{(e)} = B_g[-1/2\ 1/2; -1/2\ 1/2];$
$\mathcal{K}_3$ *matrix corresponding to the* η
$\mathcal{K}_3^{(e)} = -\omega . l_e .[1/3\ 1/6; 1/6\ 1/3];$
Overall stiffness matrix
$\mathcal{K}^{(e)} = \mathcal{K}_1^{(e)} + \mathcal{K}_2^{(e)} + \mathcal{K}_3^{(e)};$
Assembling global stiffness matrix, $\mathcal{K}_{Glob}$
$for\ i = 1 : n_e + 1$
$for\ j = 1 : n_e + 1$
$if\ (i == j)$
$if(i == 1)$
$\mathcal{K}_{Glob_{i,j}} = \mathcal{K}_{1,1}^{(e)};$
$elseif(i == n_e + 1)$
$\mathcal{K}_{Glob_{i,j}} = \mathcal{K}_{2,2}^{(e)};$
$else$
$\mathcal{K}_{Glob_{i,j}} = \mathcal{K}_{1,1}^{(e)} + \mathcal{K}_{2,2}^{(e)};$
end
$elseif(i == j + 1)$
$\mathcal{K}_{Glob_{i,j}} = \mathcal{K}_{1,2}^{(e)};$
$elseif(j == i + 1)$
$\mathcal{K}_{Glob_{i,j}} = \mathcal{K}_{2,1}^{(e)};$
$else$
$\mathcal{K}_{Glob_{i,j}} = 0;$
end
end
end
$for\ i = 2 : n_e + 1$ {*Continue assembling* $\mathcal{K}_{Glob}$}
$\mathcal{K}_{Glob_{1,i}} = 0;$ {*Striking the first and the last rows*}
$\mathcal{K}_{Glob_{n_e+1,i}} = 0;$
end
$\mathcal{K}_{Glob_{1,1}} = 1;$
$\mathcal{K}_{Glob_{n_e+1,n_e+1}} = 1;$
$f_{1,1} = \eta_1;$ {Applying BC, $\eta(t_1) = \eta_1$}
$f_{ne+1,1} = \eta_2;$ {Applying BC, $\eta(t_2) = \eta_2$}
$[\eta] = [\mathcal{K}_{Glob}]^{-1}.[f];$ {Solving for η}
$for\ i = 1 : n_e$
$d\eta_i = (\eta_{i+1} - \eta_i)/l_e;$ {Calculating $\dot{\eta}$}
end
$for\ i = 2 : ne$
$d^2\eta_i = (d\eta_{i+1} - d\eta_i)/l_e;$ {Calculating$\ddot{\eta}$}
end

$$\begin{bmatrix} 1 & 0 & 0 & . & . & 0 \\ \boldsymbol{\mathcal{K}}_{21}^{(1)} & \boldsymbol{\mathcal{K}}_{22}^{(1)} + \boldsymbol{\mathcal{K}}_{11}^{(2)} & \boldsymbol{\mathcal{K}}_{12}^{(2)} & . & . & 0 \\ 0 & \boldsymbol{\mathcal{K}}_{21}^{(2)} & \boldsymbol{\mathcal{K}}_{22}^{(2)} + \boldsymbol{\mathcal{K}}_{11}^{(3)} & . & . & 0 \\ . & . & . & . & . & . \\ 0 & 0 & 0 & . & 0 & 1 \end{bmatrix}_{n_d \times n_d} \cdot \begin{Bmatrix} \eta_1 \\ \eta_2 \\ \eta_3 \\ . \\ . \\ \eta_n \end{Bmatrix}_{n_d \times 1} = \begin{Bmatrix} \eta(t_1) \\ 0 \\ 0 \\ . \\ . \\ \eta(t_2) \end{Bmatrix}_{n_d \times 1}$$

$$[\boldsymbol{\mathcal{K}}_{Glob}]_{n_d \times n_d} . \{\boldsymbol{\eta}\}_{n_d \times 1} = \{\eta(t_1) \quad 0 \quad 0 \quad . \quad . \quad \eta(t_2)\}^T_{n_d \times 1} \tag{9}$$

Table 3: System parameters values

Parameters	Values
$\omega_1\ (Hz)$	2.7340
$\omega_2\ (Hz)$	7.4840
$X_{1,1}\ (m)$	1
$X_{1,2}\ (m)$	1.2890
$X_{2,1}\ (m)$	1
$X_{2,2}\ (m)$	-1.4645
$\phi_{1,1}\ (m)$	0.7753
$\phi_{1,2}\ (m)$	1
$\phi_{2,1}\ (m)$	1
$\phi_{2,2}\ (m)$	-1.4645
$M_1\ (kg)$	480.4600
$M_2\ (kg)$	907.5400
$K_1\ (N.m^{-1})$	3593.4000
$K_2\ (N.m^{-1})$	50834
$\tilde{\phi}_{1,1}\ (m)$	0.0354
$\tilde{\phi}_{1,2}\ (m)$	0.0456
$\tilde{\phi}_{2,1}\ (m)$	0.0332
$\tilde{\phi}_{2,2}\ (m)$	-0.0486
$Bg_{1,1}(N.s.m^{-1})$	0.0034
$Bg_{1,2}\ (N.s.m^{-1})$	-0.0156
$Bg_{2,1}\ (N.s.m^{-1})$	-0.0156
$Bg_{2,2}\ (N.s.m^{-1})$	0.1349
$Kg_1\ (N.m^{-1})$	7.4789
$Kg_2\ (N.m^{-1})$	56.0126
$Bg_{diag1}\ (N.s.m^{-1})$	1.0061
$Bg_{diag2}\ (N.s.m^{-1})$	38.9460
$\zeta_1\ (N.s.m^{-1}/Hz)$	0.1839
$\zeta_2\ (N.s.m^{-1}/Hz)$	2.6019

RESULTS

The two uncoupled modal equations were solved through both numerical algorithms in Table 1 and 2 with numerical values provided in Table 3. The two algorithms showed no significant difference when used for small time frames, however, as mentioned earlier, when number of terms increases in the first algorithm, the power of the trial functions also ascends linearly. In order to examine the behavior of the suspension system under no force, the second algorithm along with modal analysis was used to calculate displacements of suspension masses as well as their velocity and acceleration in a time frame of 5 sec and in the presence and absence of damping. Plots of the responses are shown in Fig. 2 to 5 for both modal equations $\boldsymbol{\eta}(t)$ and $\mathbf{x}(t)$. For the damped case (Fig. 4 and 5), where vibrations are ultimately damped to zero, asymptotic or exponentially stability is observed. To determine a conclusive result, we define $\mathrm{X} = (\mathrm{x}_1, \mathrm{x}_2) = (\mathbf{x}, \dot{\mathbf{x}})$ as the state of the system, where $d/dt[\boldsymbol{x}_1 \quad \boldsymbol{x}_2]^T = [\boldsymbol{x}_1 \quad -(\boldsymbol{K}/\boldsymbol{M})\boldsymbol{x}_1 - (\boldsymbol{B}/\boldsymbol{M})\boldsymbol{x}_2]^T$. To check the stability of this system, we proceed with the Lyapunov's direct method by considering the energy of the system as the Positive Definite (PD), continuously differentiable candidate Lyapunov function given by $V(\mathbf{X}, \boldsymbol{t}) = \frac{1}{2}\mathbf{M}\boldsymbol{x}_2^2 + \frac{1}{2}\mathbf{K}\boldsymbol{x}_1^2$. Therefore, direct differentiation of this

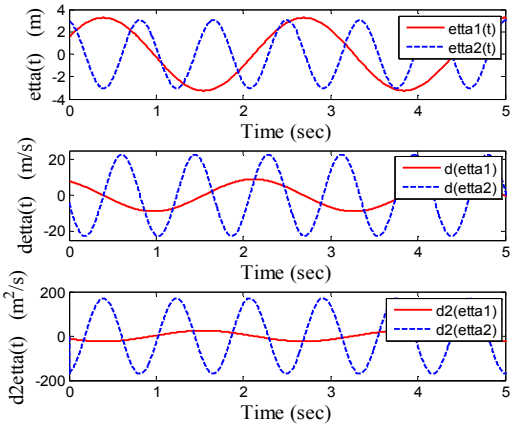

Fig. 2: Plots of modal responses, $\eta_1(t)$, $\eta_2(t)$, $\dot{\eta}_1(t)$, $\dot{\eta}_2(t)$, $\ddot{\eta}_1(t)$ and $\ddot{\eta}_2(t)$ for zero damp case

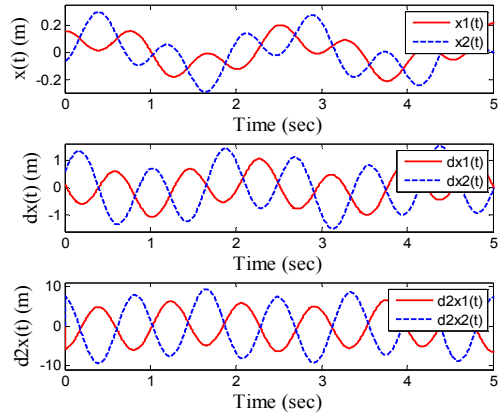

Fig. 3: Plots of system responses, $x_1(t)$, $x_2(t)$, $\dot{x}_1(t)$, $\dot{x}_2(t)$, $\ddot{x}_1(t)$ and $\ddot{x}_2(t)$ for zero damp case

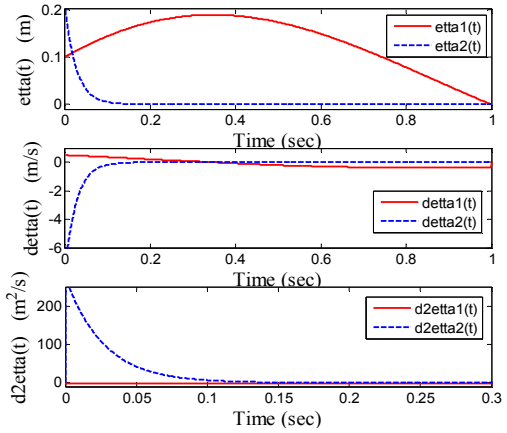

Fig. 4: Plots of modal responses, $\eta_1(t)$, $\eta_2(t)$, $\dot{\eta}_1(t)$, $\dot{\eta}_2(t)$, $\ddot{\eta}_1(t)$ and $\ddot{\eta}_2(t)$ for damped case

function along trajectories of the original system yields: $\dot{V}(\boldsymbol{X},\boldsymbol{t}) = \mathbf{M}\boldsymbol{x}_2\dot{\boldsymbol{x}}_2 + \mathbf{K}\boldsymbol{x}_1\boldsymbol{x}_2$. We can re-write $\dot{V}$ as $\dot{V}(\boldsymbol{X},\boldsymbol{t}) = -\mathbf{B}\boldsymbol{x}_2^2$ to confirm that the function $-\dot{V}(\boldsymbol{X},\boldsymbol{t})$ does not depend on x_1, hence it is quadratic but not locally positive definite and we cannot conclude

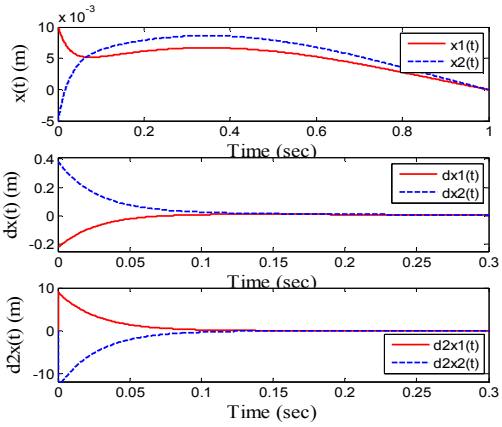

Fig. 5: Plots of system responses, $x_1(t)$, $x_2(t)$, $\dot{x}_1(t)$, $\dot{x}_2(t)$, $\ddot{x}_1(t)$ and $\ddot{x}_2(t)$ for damped case

exponentially stability, however by using Lassalle's invariance principle, asymptotic stability can be concluded. If we define the PD function:

$$V(\mathbf{X},\boldsymbol{t}) = \frac{1}{2}[\boldsymbol{x}_1 \quad \boldsymbol{x}_2]\begin{bmatrix} K & \epsilon M \\ \epsilon M & M \end{bmatrix}[\boldsymbol{x}_1 \quad \boldsymbol{x}_2]^T$$

where, ϵ is a very small positive constant, the derivative of the Lyapunov candidate would be:

$$\dot{V}(\boldsymbol{X},\boldsymbol{t}) = -[\boldsymbol{x}_1 \quad \boldsymbol{x}_2]\begin{bmatrix} \epsilon\mathbf{K} & \frac{1}{2}\epsilon\mathbf{B} \\ \frac{1}{2}\epsilon\mathbf{B} & \mathbf{B}-\epsilon\mathbf{M} \end{bmatrix}[\boldsymbol{x}_1 \quad \boldsymbol{x}_2]^T$$

We can now see that by choosing of sufficiently small values of ϵ, the function $\dot{V}(X,t)$ can be made negative definite and exponential stability can be concluded as shown in figure.

CONCLUSION

This study discussed development of an implementable algorithm for assessing the performance of a two-degree of freedom tractor active suspension model under free vibrations. The natural frequencies, amplitudes of the motions, normal modes, generalized mass, stiffness and damping matrices, re-normalized normal modes, diagonalized damping matrix and effective modal damping factors were determind. Because the original vertical equations of motion in physical coordinates were coupled, they were first projected onto modal coordinates. Each modal equation was then solved independently through Galerkin's method over same size elements of time domain. The numerical results from modal Eq. (4) and (5) were then transformed back to physical coordinates to construct the response of the actual system given by Eq. (3). The results were plotted for both no-damp and damped case to show the effectiveness of the implemented numerical method in solving the two-DOF suspension system. For the damped case, since the asymptotic or exponentially

stability behavior of response could not be exactly determined from response plot of x(t), the Lyapunov's direct method was applied and exponential stability was concluded.

REFERENCES

Carson, W.M., K.C. Watts and S.N. Sarwal, 1979. Galerkin's method in agricultural engineering. Can. Agric. Eng., 21: 125-130.

Deboli, R. and S. Potecchi, 1986. Determination of the behavior of seats for agricultural machines by means of vibrating bench. Proceeding of the AIGR Meeting and Infortunistica. Firenze, December 2-3, pp: 233-238.

Dormand, J.R. and P.J. Prince, 1980. A family of embedded Runge-Kutta formulae. J. Comput. Appl. Math., 6: 19-26.

Hansson, P.A., 1995. Optimization of agricultural tractor cab suspension using the evolution method. Comput. Electron. Agr., 12: 35-49.

Hansson, P., 1996. Rear axle suspensions with controlled damping on agricultural tractors. Comput. Electron. Agr., 15: 123-147.

Hilton, D.J. and P. Moran, 1975. Experiments in improving tractor operator ride by means of a cab suspension. J. Agric. Engng. Res., 20(4): 433-448.

Kantorovich, L.V. and V.I. Krylov, 1964. Approximate Methods of Higher Analysis. John Wiley & Sons, New York.

Kolator, B. and I. Białobrzewski, 2011. A simulation model of 2WD tractor performance. Comput. Electron. Agr., 76(2): 231-239.

Lehtonen, T. and M. Juhala, 2006. Predicting the ride behaviour of a suspended agricultural tractor. Int. J. Vehic. Syst. Mod. Test., 1(1-2): 131-142.

Lines, J., M. Stiles and R. Whyte, 1995. Whole body vibration during tractor driving. J. Low Frequen. Noise Vib., 14(2): 87-104.

Matthews, J., 1964. Ride comfort for tractor operator II: Analysis of ride vibration on pneumatic-tyred tractors. J. Agric. Eng. Res., 9(2): 147-158.

Matthews, J., 1977. The ergonomics of tractors. ARC Res. Rev., 3(3): 59-65.

Marsili, A., L. Ragni, G. Santoro and G. Servadio, 2002. Innovative systems to reduce vibrations on agricultural tractors: comparative analysis of acceleration transmitted through the driving seat. Biosyst. Eng., 81(1): 35-47.

Mehta, C. and V. Tewari, 2000. Seating discomfort for tractor operators-a critical review. Int. J. Ind. Ergonom., 25(6): 661-674.

Mehta, C.R., L.P. Gite, S.C. Pharade, J. Majumder and M.M. Pandey, 2008. Review of anthropometric considerations for tractor seat design. Int. J. Ind. Ergonom., 38(5-6): 546-554.

Mothiram, K.P. and M.S. Palanichamy, 1985. Minimization of human body responses to low frequency vibration: Application to tractors and trucks. Math. Mod., 6(5): 421-442.

Nocedal, J. and S.J. Wright, 2006. Numerical Optimization. 2nd Edn., Springer Verlag, New York.

Park, W. and J.R.R. Stott, 1990. Response to vibration. 137: 545-546.

Patil, M.K. and M.S. Palanichamy, 1988. A mathematical model of tractor-occupant system with a new seat suspension for minimization of vibration response. Appl. Math. Mod., 12(1): 63-71.

Rossegger, R. and S. Rossegger, 1960. Health effects of tractor driving. J. Agric. Eng. Res., 5(3): 241-274.

Roy, R.C. and J.K. Andrew, 2011. Fundamentals of Structural Dynamics. John Wiley & Sons, ISBN: 10-0470481811.

Scarlett, A.J., J.S. Price and R.M. Stayner, 2007. Whole-body vibration: Evaluation of emission and exposure levels arising from agricultural tractors. J. Terramech., 44(1): 65-73.

Servadio, P., A. Marsili and N.P. Belfiore, 2007. Analysis of driving seat vibrations in high forward speed tractors. Biosyst. Eng., 97(2): 171-180.

Shampine, L.F., M.W. Reichelt and J. Kierzenka, 2000. Solving Boundary Value Problems for Ordinary Differential Equations in MATLAB with bvp4c. Retrieved from: http:// 200.13. 98.241/ ~martin/ irq/tareas1/ bvp_paper.pdf, (Accessed on: January 0, 2012).

Stayner, R.M., 1972. Aspects of the development of a test code for tractor suspension seats. J. Sound Vib., 20(2): 247-252.

Stayner, R.M., 1976. Vibration of the tractor on march and human body response. Cars Motoriagricoli (Italian), 2: 37-43.

Stayner, R.M., T.S. Collins and J.A. Lines, 1984. Tractor ride vibration simulation as an aid to design. J. Agric. Engng. Res., 29: 345-355.

Thoresson, M.J., 2003. Mathematical optimisation of the suspension system of an off-road vehicle for ride comfort and handling. M.A. Thesis, University of Pretoria, Pretoria.

Yang, Y., W. Ren, L. Chen, M. Jiang and Y. Yang, 2009. Study on ride comfort of tractor with tandem suspension based on multi-body system dynamics. Appl. Math. Modell., 33(1): 11-33.

Zehsaz, M., M.H. Sadeghi, M.M. Ettefagh and F. Shams, 2011. Tractor cabin's passive suspension parameters optimization via experimental and numerical methods. J. Terramech., 48(6): 439-450.